Development of Multi-Disciplinary Simulation Codes and their Application for the Study of Future Space Transport Systems

Yukimitsu. Yamamoto
JAPAN Aerospace Exploration Agency

Keywords: *Numerical Simulation, Aerodynamics, Space Transport*

Abstract

Numerical simulation technology enlarges its application area with the progress of the computer hardware systems and has been developed as the strong aerodynamic design tools which cover all flight range of space transport system from the launching to the re-entry flight.

In the present study, multi-disciplinary simulation codes have been applied for the design of the future TSTO systems.

CFD codes are coupled with the unsteady motions of the six degree of freedom and HSFD Phase II flights are being reconstructed.

Plume interactions are investigated, where CFD for external flow is coupled with the internal nozzle flow computations. Shock interactions in the ascent phase of TSTO rocket are also analyzed and simulations of second stage orbiter separation are now progressed.

Flow-thermal structural coupling for TPS are conducted for HYFLEX re-entry flight experiments and re-building of aerothermal environments of the HYFLEX flight has been accomplished.

Through these applications of the present multi-disciplinary simulation codes, it is indicated that various design problems for future TSTO space transport systems can be resolved efficiently.

1 Introduction

The TSTO launching system has come to be considered a main candidate for next generation space transport systems. CFD has played a very important role in the aerothermodynamic design of atmospheric flight vehicles such as HOPE-X and HYFLEX [1]~[8]. In order to develop our CFD technology in another practical and useful area, we have pursued the study of multi-disciplinary simulations based on JAXA ITBL (Internet Based Laboratory) projects. Fig.1 shows an image of a next generation TSTO system for space exploration. Our objective is to construct a multi-disciplinary design system that simulates flight of the next generation TSTO from launch to final landing approach. In near future, it will be especially important to predict and avoid several risks that arise in TSTO space flight and to construct optimum system designs using concurrent engineering methods.

In developing these space transport systems, important aerodynamic problems, which must be investigated, are depicted in Fig.2, from the

Fig.1 Image of Next Generation TSTO Rocket System for Manned Space Exploration

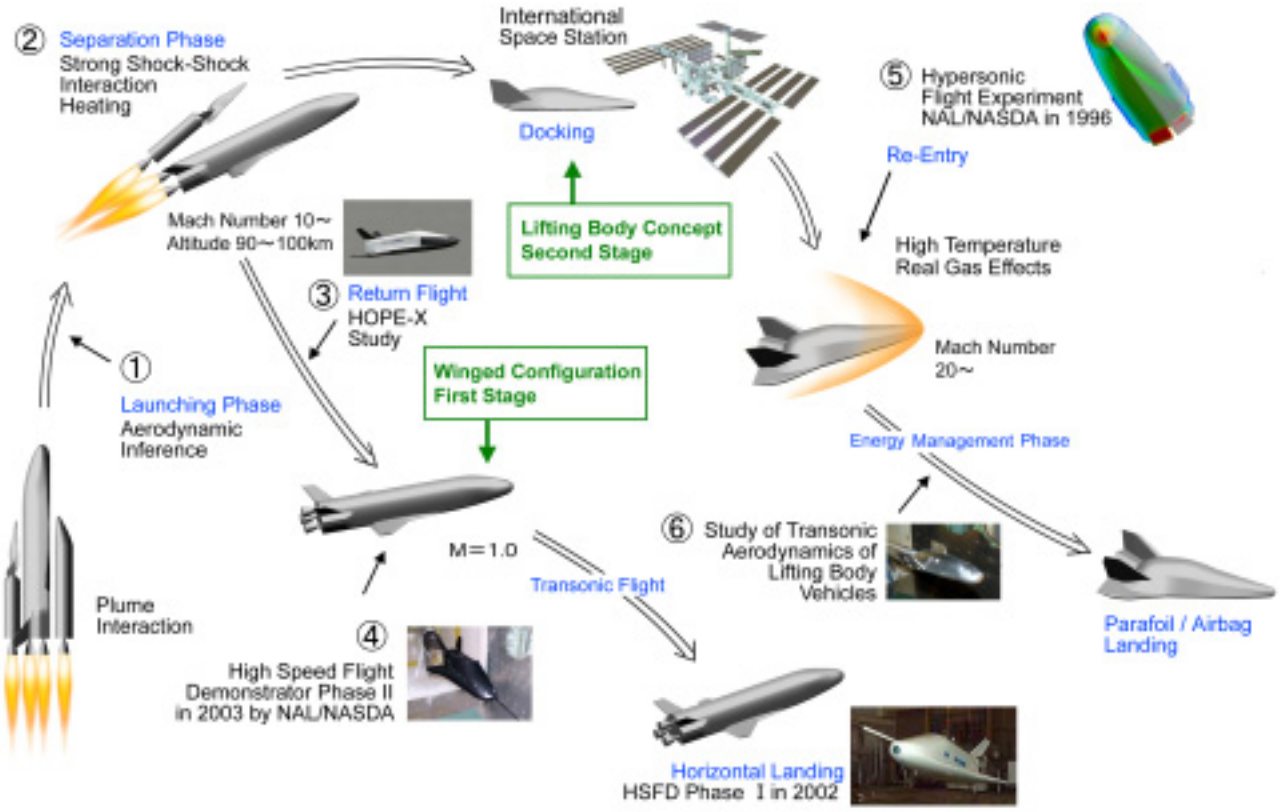

① Basic Validation of Hypersonic Shock-Shock Interaction Problem for TSTO Systems
② Analysis of TSTO Hypersonic Separation
③ Re-entry Flight Analysis of HOPE-X Winged Body Configuration
④ High Speed Flight Demonstrator Phase II Experiment for the Evaluation of Transonic Aerodynamics
⑤Evaluation of HYFLEX (Hypersonic Flight Experiment) Re-Entry Flight
⑥ Study of Subsonic, Transonic and Supersonic Aerodynamics of Lifting Body Type

Fig.2 Related Studies for TSTO Space Transport Systems consisting of Lifting and Winged Body Concepts

launching to final landing phase of the vehicle through atmospheric re-entry flight. In the figure, are also inserted the related studies conducted through HOPE-X project [1]～[6], which has been continued for more than one decade. In the HOPE-X development phase, several flight experiments have been made such as HYFLEX for hypersonic lifting body re-entry research [7],[8], HSFD phase I for the automatic horizontal landing technology and HSFD phase II for transonic aerodynamics investigations [9],[10]. Recently, configuration design study of the lifting body vehicles has started and re-entry aerodynamics have been investigated from subsonic to hypersonic regions [11],[12]. In the present report, we introduce recent studies of the aerodynamics of these future space transport vehicles.

2 Multi-Disciplinary Simulation of Next Generation Space Transport Vehicles

2.1 HSFD (High Speed Flight Demonstrator) Phase II Transonic Aerodynamics

The HSFD (High Speed Flight Demonstration) Phase II flight experiment was conducted to reduce uncertainties in the transonic aerodynamic characteristics predicted by the wind tunnel tests and CFD simulations [9],[10].

In Fig.3, mission profile is illustrated. A test vehicle is lifted to high altitude by balloon system to allow it to accelerate to transonic speeds in free-fall. After release, the vehicle

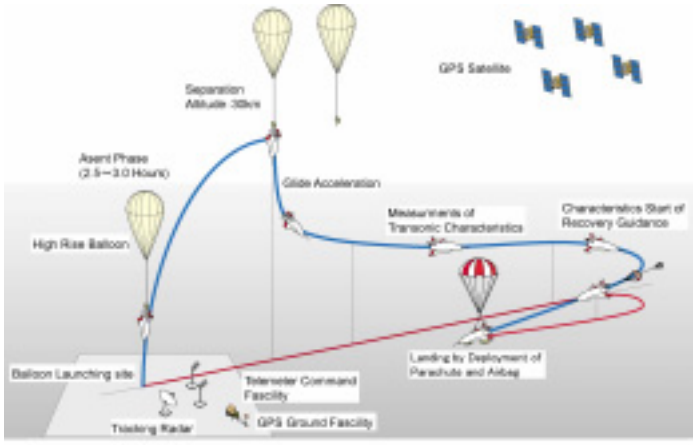

Fig.3 HSFD Phase II Mission Profile

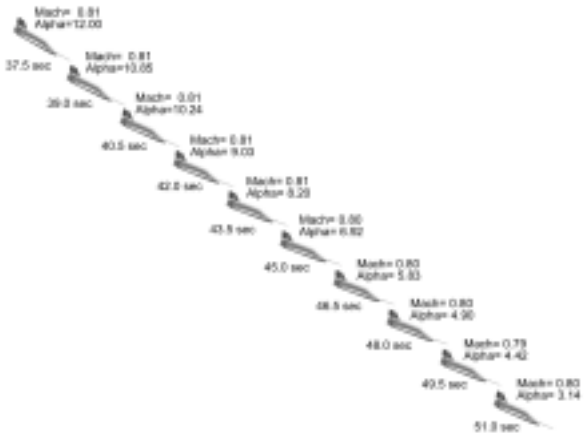

Fig.4 HSFD M_∞=0.8 Flight Profile

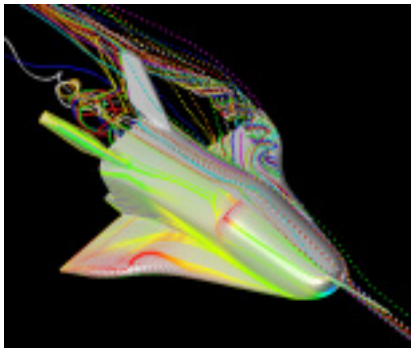

M_∞=0.81, δelv=8.7°, Re_∞=9.37X10^6
a) α=12°

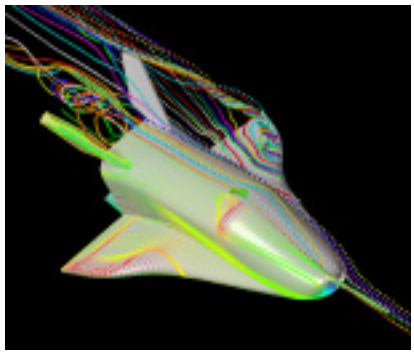

M_∞=0.81, δelv=9.2°, Re_∞=1.07X10^7
b) α=8°

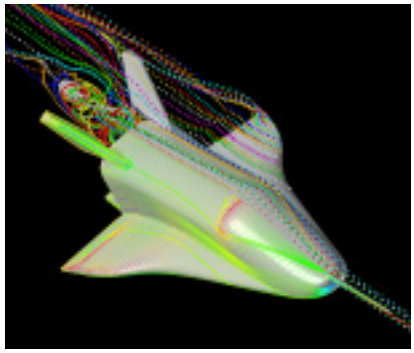

M_∞=0.8, δelv=9.0°, Re_∞=1.17X10^7
c) α=4°

Fig.5 Streamline Patterns of HSFD Phase II Flight Conditions at M_∞=0.8

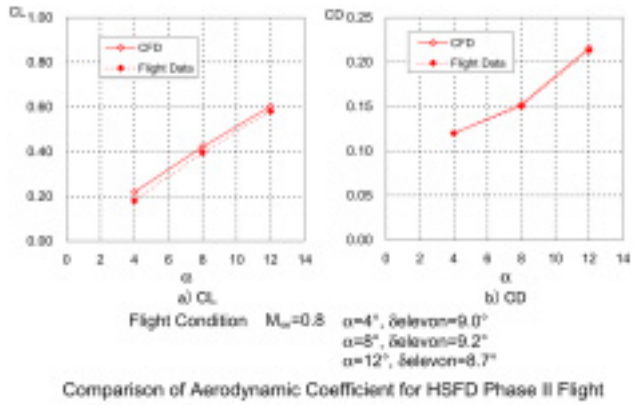

Fig.6 Comparison of Aerodynamic Coefficients for HSFD Phase II Flight

can fly at a constant Mach number while changing its angle of attack quasi-statically, and its trimmed aerodynamic characteristics will be estimated from the obtained flight data. Phase II flight experiment was conducted in collaboration with Centre National d' Etudes Spatiales (CNES) at the Swedish Space Corporation's Esrange site in Sweden in July 2003.

In HSFD Phase II experiment, flight data was obtained at M_∞=0.8. The flight profile and attitude of HSFD vehicle are illustrated in Fig.4. The angle of attack changes from 12 to 4 deg during the constant Mach number flight at M_∞ =0.8. The flight time is about 15 seconds and elevons are deflected about 9 deg. to take trim stability during this flight. CFD computations are made for the typical 3 cases at angles of attack α=12°, 8° and 4° with the flight Reynolds number of about 1 x 10^7. Oil flow patterns and three dimensional streamlines are depicted in Fig.5. It is clearly found that the wing tip vortex is generated at high angle of attack at

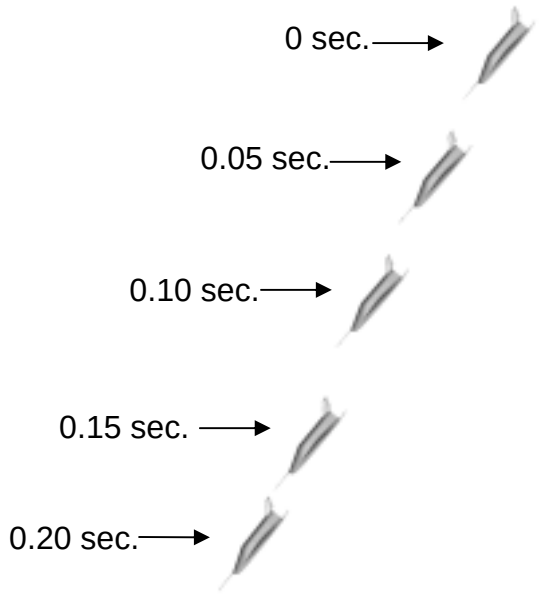

Fig.7 Transonic Re-Entry Flight Simulation of HSFD from CFD with Equations with 6 deg. of Freedom of Motion (Test Case for M_∞=1.05 Flight)

α=12° and disappears gradually with decreasing the angle of attack. Comparisons of lift and drag coefficients with the flight data are shown in Fig.6. Excellent agreements are obtained for the drag coefficient and evaluations for the lift coefficients can be made sufficiently.

Then, CFD computations are coupled with equations of 6 degrees of freedom motion and transonic unsteady flight of the HSFD can be simulated.

Fig.7 shows the preliminary numerical results for the HSFD trajectory. For the complete flight analysis, computations have been continued and more accurate flight evaluations are in progress.

2.2 Plume Interaction Analysis

Plume interactions are important problems for the rocket propelled TSTO systems. Especially, multi-nozzle flows must be analyzed precisely to avoid unfavorable interferences when the nozzles are operated to control the flight attitude of the vehicle. Typical results of plume effect analysis are shown in Fig.8 and 9, where multi block Navier-Stokes computations have been performed in the transonic ascent phase of the wing body model. In the present analysis, HOPE 11 geometry is applied for the typical case of the TSTO first stage ascent flight.

In Fig.10, 11 and 12 are shown the computational results of the next generation main rocket planned in future succeeding to the present H2A launching system.

Here, the cluster nozzle problems are focused on and preliminary analysis starts for hypersonic plume interaction flow fields.

Surface Mesh is presented in Fig.10. Four cluster nozzles are combined in main rocket body with the two solid rocket boosters. Present configurations are determined tentatively for preliminary computations.

Streamlines of forward part of the main rocket

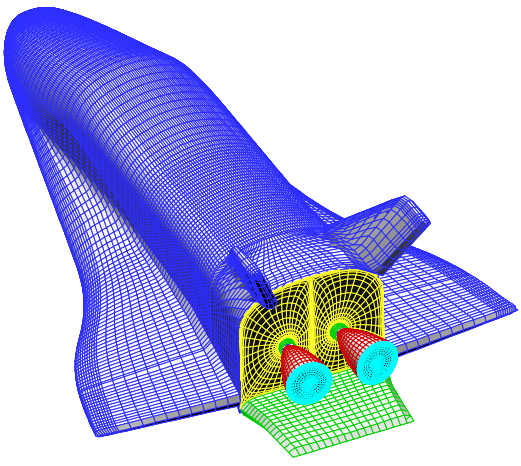

Fig.8 Surface Mesh of HOPE 11 for Nozzle Flow Analysis

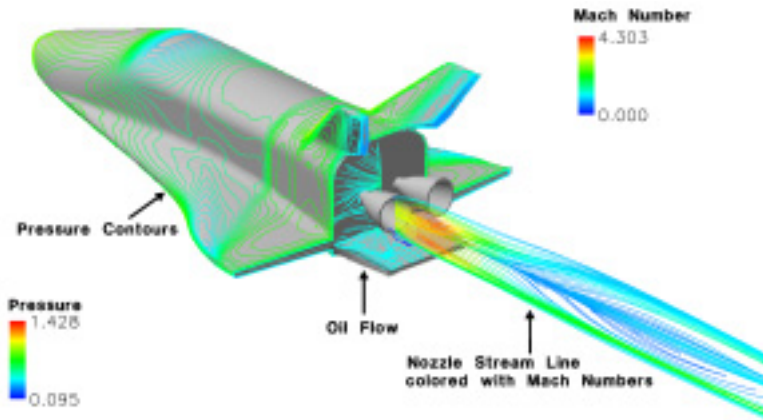

Fig.9 Nozzle Plume Interaction Analysis

Main Flow condition

M_∞=1.05, Re_∞=4.16x107, α=10deg, P_∞=12kpa, T_∞=273K

Nozzle Exit Condition

M_∞=3.0, P_∞=24kpa, T_∞=1071K

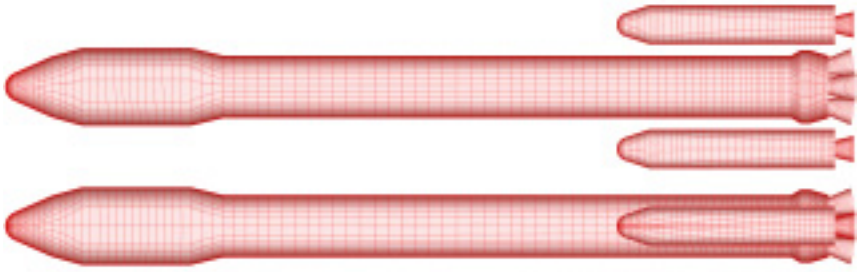

Fig.10 Planned Configuration of Next Japanese Main Rocket System

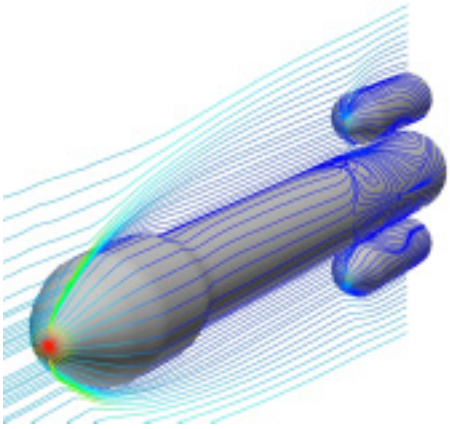

Fig.11 Forward Interaction Flow Field Analysis with Solid Rocker Boosters (M_∞=10.0, α=0deg)

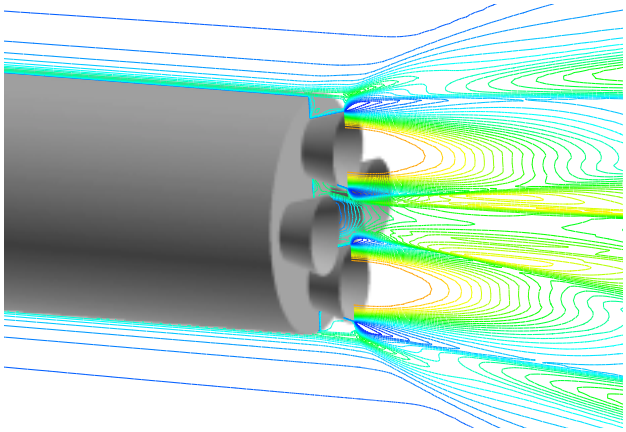

Fig.12 Cluster Nozzle Interaction Analysis

External Flow Condition M_∞=4.06, T_∞=258, Re_∞=1.07x10^7
Nozzle Exit Condition M_n=5.35, T_n=985, P_e / P_∞=16.86

are plotted in Fig.11 at M_∞=10.0 and α=0deg. Shock interactions which occur between the main rocket body and SRB are investigated in detail.

For these interaction flows, preliminary validation has been already made, using two hemisphere cylinders, and aerodynamic heating is predicted quantitatively well, compared with JAXA HWT infrared heat transfer measurements [13].

In Fig.12 are plotted pressure contours around the cluster nozzles of the next generation main rocket system. External flow and nozzle exit conditions are determined temporally. At present, no severe interactions can be observed at the normal conditions.

2.3 Combined Study of Hypersonic Aerodynamic Interference in TSTO Ascent Flight

Important aerodynamic problems in the TSTO ascent flight are shock-shock or shock-boundary layer interactions, which occur between the first-stage vehicle and the boosters or in the separation phase of the first- and second-stage vehicles. In order to investigate these complicated flowfields, a study using both CFD and HWT has been undertaken at the JAXA [14]. Fig.13 shows a model in place and typical shock interaction features can be observed in the shadowgraphs of Figure 14. Fig.15 shows comparisons of oil flow patterns on the booster nose area. Complex shock interaction flow structures are captured well. Quantitative comparisons of heat transfer distribution on the booster nose are made in Fig.16, where excellent agreement is obtained with local peak heating characteristics. Heat transfer measurements were made by the infrared systems at JAXA HWT. Finally, a numerical study of TSTO separations is presented. In Fig.17 (a), the separations of two ellipsoids are shown at M_∞ = 2.0. Overset moving grids are used and the numerical scheme is based on the AUSM-DV, using 3D Navier-Stokes equations. In Fig.17 (b) TSTO separation analyses are made. Strong shock interactions are revealed on the second stage nose at an inclination angle of 10° .

Fig.13 TSTO Model in NAL M10 HWT

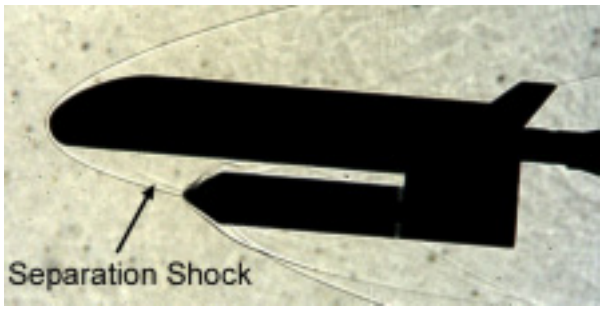

Fig.14 Shadowgraph (M_∞=9.58, α=10°)

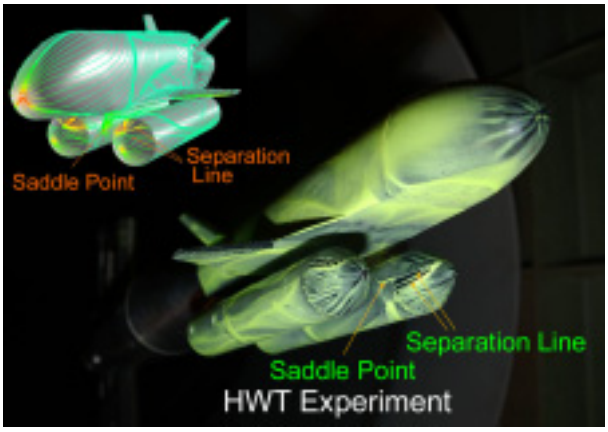

Fig.15 Comparison of Oil Flow Patterns on the Booster Nose (M_∞=9.58, α= 10°)

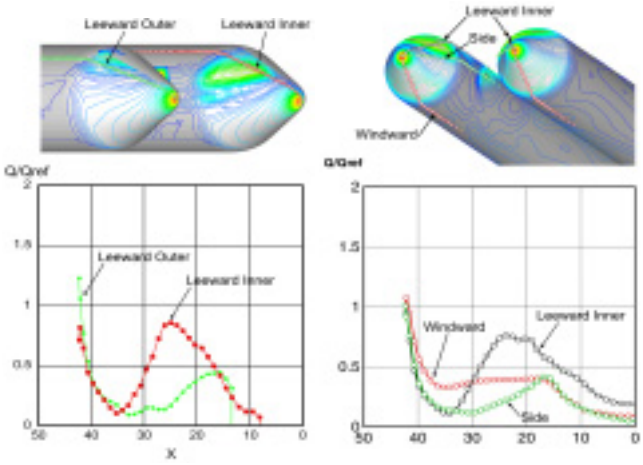

a) Experiment b) Computation

Fig.16 Comparison of Heat Transfer Distributions on the Boosters Nose (M_∞=9.58, α=10deg)

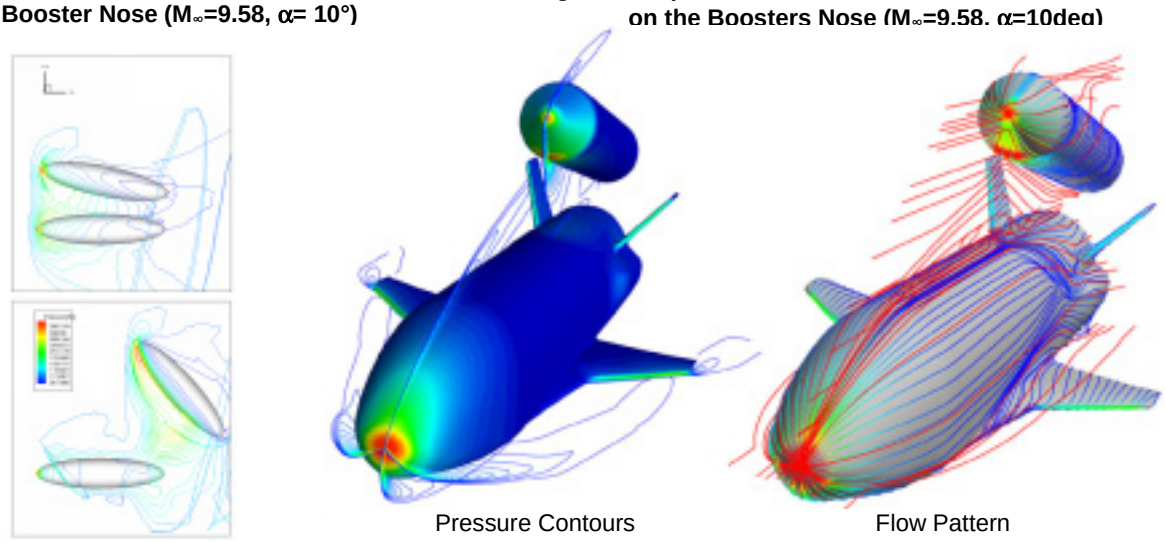

Pressure Contours Flow Pattern

a) Basic Research of Separation Motion at M_∞=2.0

b) TSTO Separation Analysis at the 10 deg Second Stage Inclination Angle (M_∞=9.58, α=0deg)

Fig.17 Numerical Study of TSTO Separation

Basic validations of the local heat transfer peak produced by the severe shock-shock interactions at this separation stage, have been performed through the comparisons with HWT infrared measurements, using two hemi-sphere cylinders. Bow shock wave from the nose of large hemi-sphere cylinder impinges on the nose of the inclined small one to induce Type III shock interactions. Detailed results are reported in Ref.15.

2.4 Re-Entry Aerothermodynamics and TPS Thermal Analysis of HYFLEX

Another multi-disciplinary application involves the design of the thermal protection system for space transport vehicles, where aerothermal structural coupling is a significant factor. These tasks are accomplished with simulations and then validated with the HYFLEX atmospheric flight experiments [8].

HYFLEX flight experiment was conducted in Feb., 1996. Figure 18 shows surface temperature history of HYFLEX flight, simulated by CFD-FEM coupling analysis [7]. In the figure, surface temperature change is demonstrated at ten seconds intervals with HYFLEX flight attitude. In hypersonic flight range from flight time 50 to 200sec., maximum nose heating is produced at the flight time of 130 sec and maximum temperature of 1450K is caused on the C/C nose stagnation region at the flight time of 150sec. CFD/FEM coupling method developed previously, can predict these phenomena.

Figure 19 shows the typical pick up results in Fig.18. Temperature distributions of the surface and internal TPS are depicted. TPS are drawn in a enlarged from to the inner direction. HYFLEX windward TPS is composed of 4mm thick C/C nose cap and 25mm thick ceramic tiles. On the C/C nose cap, aerodynamic heating was measured at five locations. In the symmetry cross section, four measurement points are arranged as shown in Fig.20. Point TA03 is located near the nose stagnation point during the initial stage of HYFLEX re-entry flight, where HYFLEX flew at a constant angle of attack of α=49deg. until the flight time of 120 sec.

Comparisons of temperature increase at these measurement points are also presented in Fig.20. As shown in the figure, present CFD/FEM coupling method simulates well with these inferred flight temperature increase. Also, temperature data obtained by using ANSYS thermal analysis software are plotted in the figure. Agreements between numerical and ANSYS results are excellent.

After the flight time of 120 sec, it is remarked that inner of the C/C nose cap. The flexible insulator attached to the bulk head is heated up and a strong reflection comes to the rear surface of the C/C nose the bulk head insulator. To take this phenomena into account, analysis using ANSYS thermal software has been made with and without the computations of the inner radiation [8]. Typical ANSYS results are presented at the flight time of 150 sec., where maximum temperature revealed on the C/C nose cap during HYFLEX re-entry flight. In Fig.21, temperature contours are depicted for the cases with and without the inner radiation. The differences of the maximum nose stagnation temperature becomes more than 100K. Temperature of the bulk head insulator increases about 1200K by this radiation effect.

2.5 Re-Entry Study of Future Space Transport

In order to investigate the capability of lifting atmospheric re-entry, a series of numerical and experimental study has been performed [12]. Especially, transonic wind tunnel tests are mainly conducted at JAXA to investigate non-linear aerodynamic characteristics.

In Fig.22, typical three dimensional streamline patterns are depicted at M_∞=0.5 and α=17deg.

Through a series of parametric design study, it is known that the transonic aerodynamics of the present lifting body configuration are greatly affected by the fin geometry. In order to reduce the fin induced nonlinearity, which accompanies vortex break down phenomena downstream, sophisticated design must be made to avoid separations at the root of the fin.

Finally, hypersonic flow simulation of the re-entry technology demonstrator is presented. In Fig.23 are shown oil flow and streamline patterns around the wing-body vehicle at M_∞ =26.0, α=50deg and β=5deg.

This vehicle may be considered as the candidate of TSTO first stage vehicle. Flight experiments are planned by vertical rocket launching in future.

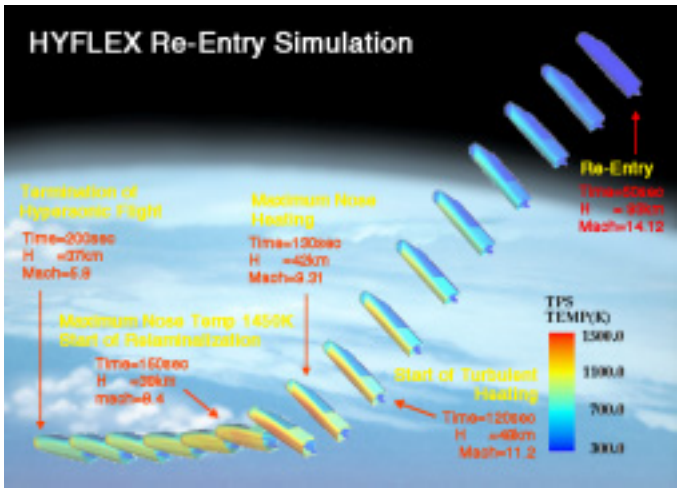

Fig.18 Aero-thermal Coupling Simulation of HYFLEX Re-Entry Flight

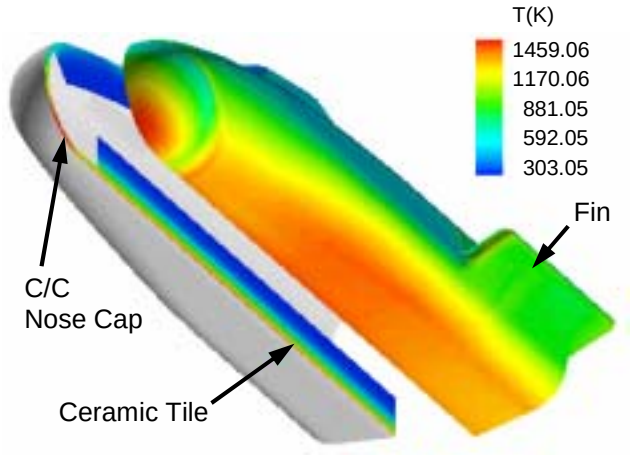

Fig.19 Surface and Internal TPS Temperature Distributions of HYFLEX

Flight Time=130 sec Altitude=42.5km
Uinf=3348.5m/sec Tinf=258K
Pinf=197.5Pa Minf=10.4

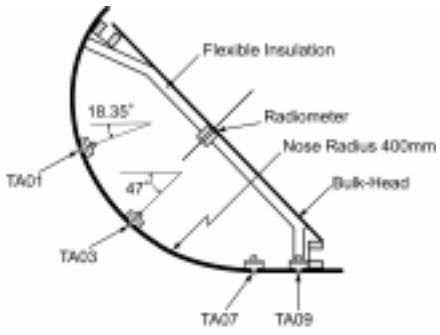

C/C Nose Cap Temperature Measurement Points

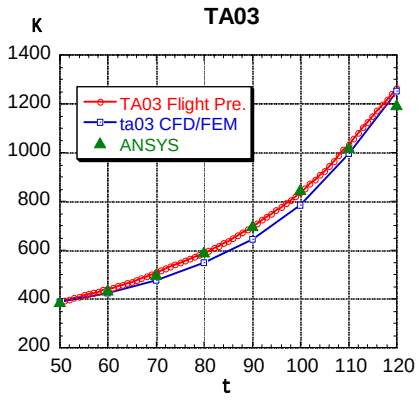

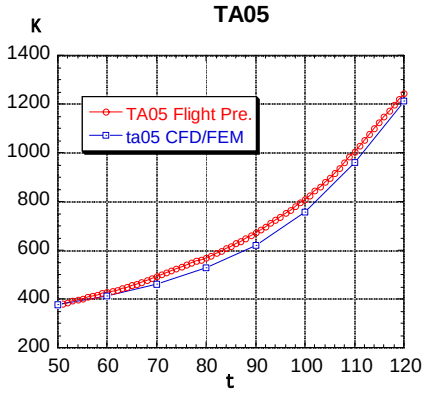

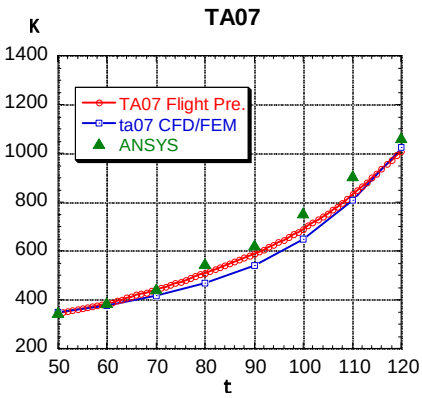

Plots of Temperature Increase

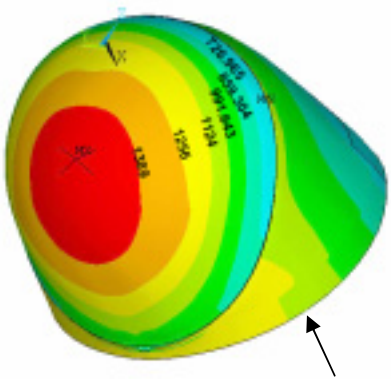

Without Inner Radiation
Maximum Temperature 1500K

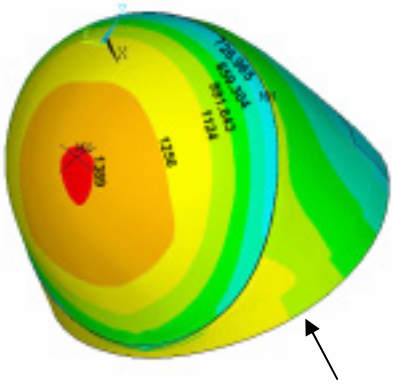

With Inner Radiation Effects
Maximum Temperature 1400K

Fig.20 Comparisons of Temperature Increase of HYFLEX C/C Nose Cap with Flight Data

Fig.21 Comparisons of Nose Temperature with and without Inner Radiation Effect

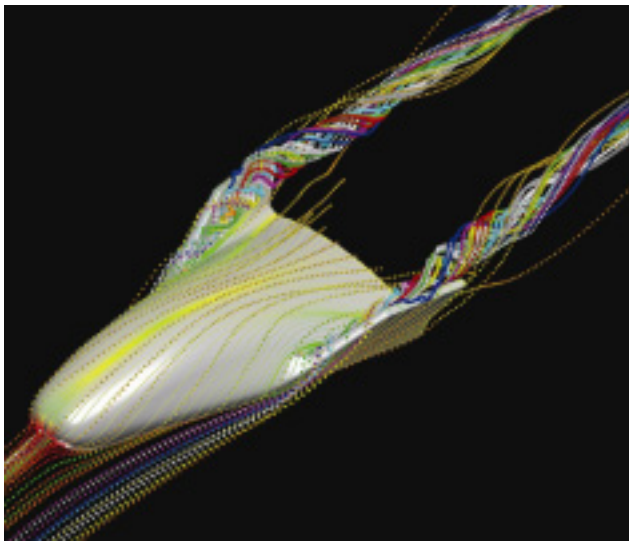

Fig.22 Flow Simulation of Lifting Body Vehicles (M_∞=0.5, R_∞=2.1x10^6, α=17deg)

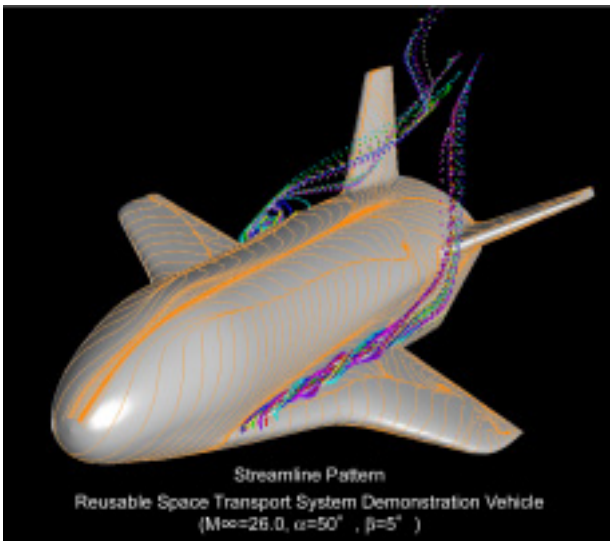

Fig.23 Hypersonic Flow Analysis for Future Re-Entry Technology Development

Conclusions

Present status and applications of the multi-disciplinary simulation codes for the next generation TSTO space transport systems are overviewed. Total flight simulation including unsteady motion, combined plume interaction and thermal-structural response, will be possible from the ascent to the re-entry phase in near future with the progress of computer hardware systems and design concept of TSTO can be constructed efficiently.

References

[1] Yamamoto. Y, Akimoto. T and Suzuki. N, "Numerical simulation of hypersonic viscous flow for the design of H-II orbiting plane (HOPE)", AIAA Paper 90-0601, 1990.

[2] Yamamoto. Y, "Numerical simulation of Hypersonic Viscous Flow for the Design of H-II Orbiting Plane (HOPE) Part II", AIAA Paper 91-1390, 1991.

[3] Yamamoto. Y, Wada. Y and Yoshioka. Y, "Hypersonic CFD analysis for the aerodynamic design of HOPE", AIAA Paper 95-1770, 1995.

[4] Yamamoto. Y and Ito. R, "CFD validation of high reynolds number transonic flows around HOPE-07 model", ISTS 2000-e-02, 22nd ISTS Symposium, May 28-June 4, 2000, Morioka, Japan.

[5] Yamamoto. Y, "CFD study and validation process of hypersonic aerodynamics for the space transport systems including HOPE-X", AIAA Paper 2001-1854, 2001.

[6] Yamamoto. Y, "Present status of computational fluid dynamic study for HOPE-X aerodynamic characteristics", Proceedings of 4th Asian Computational Fluid Dynamics Conference, September 19-21, 2000, Mianyang, China.

[7] Yamamoto. Y, "Numerical analysis of hypersonic aerodynamics for atmospheric re-entry problems of HOPE and HYFLEX", AIAA Paper 98-0277, 1998.

[8] Yamamoto. Y, Kai. T and Hozumi. K, "Numerical rebuilding of aerothermal environments and CFD analysis of post flight wind tunnel tests for hypersonic flight experiment HYFLEX", AIAA Paper 2001-2899, 2001.

[9] Yamamoto. Y, Ueno. M, Yanagihara. M, Miyazawa. Y and Ito. R, "Pre-flight CFD analysis of high speed flight demonstrator phase II vehicle and the validation of HOPE-X transonic aerodynamics", AIAA Paper 2002-0685, 2002.

[10] Yamamoto. Y, M. Ueno, M. Yanagihara, Y. Miyazawa and R. Ito, "Pre-flight CFD

analysis of high speed flight demonstrator phase II vehicle and numerical estimation of aerodynamic uncertainties through the comparisons with the transonic wind tunnel experiments", ISTS 2002-e-50, 23rd ISTS Symposium, May 26-June 2, 2002, Matsue, Japan.

[11] Yamamoto. Y, Kawato. h, Watanabe. S and Fujii. K, "CFD design study of aerodynamics characteristics of atmospheric lifting body re-entry vehicles from M_∞=0.5 to 4.0", ISTS 2002-e-29, 23rd ISTS Symposium, May 26-June 2, 2002, Matsue, Japan.

[12] Yamamoto. Y, Totsuka. A, Yoshida. M, Ueno. M, Kawato. H, Hokiyama. K, Ishiyama. T and Hosaka. Y, "Progress of transonic flow simulation in the analysis of HSFD phase II flight experiment and the design problems of the lifting body re-entry vehicles", ISTS 2004-e-12, 24th ISTS Symposium, May 30-June 6, 2004, Miyazaki, Japan.

[13] Yamamoto. Y, Totsuka. A, Hozumi. K, Kaneda. M, Kamishikiryo. S, Kobayakawa. S., Hosaka. Y, "Numerical and experimental aerodynamics of strong hypersonic shock-shock interactions", AIAA Paper 2002-2891, June, 2003

[14] Yamamoto. Y, Totsuka. A, Ishiyama. T, Kaneda. M, Yoshikura. H, Hosaka. Y, Kobayakawa. S, Kamishikiryo. S and Kinoshita. T, "Study of complex three-dimensional hypersonic shock interactions for future re-usable space transport system", AIAA Paper 2003-3900, 2003.

[15] Yamamoto. Y, et al, "CFD analysis and wind tunnel experiments of hypersonic shock-shock interaction heating for two hemi sphere cylinder problem", AIAA paper 2002-0217, January, 2002